# High Bandwidth Tilt Measurement Using Low Cost Sensors

John Leavitt, Athanasios Sideris, James E. Bobrow
Department of Mechanical and Aerospace Engineering
University of California, Irvine
Irvine, CA 92697
{leavittj, asideris, jebobrow}@uci.edu

***Abstract*— In this paper a state estimation technique is developed for sensing inclination angles using relatively low cost sensors. A low bandwidth tilt sensor is used along with an inaccurate rate gyro to obtain the measurement. The rate gyro has an inherent bias along with sensor noise. The tilt sensor uses an internal pendulum and therefore has its own slow dynamics. These sensor dynamics were identified experimentally and combined to achieve high bandwidth measurements using an optimal linear state estimator. Potential uses of the measurement technique range from robotics, to rehabilitation, to vehicle control.**

## I. INTRODUCTION

Many modern mechanical control systems use orientation feedback relative to an inertial reference frame. For systems connected to the ground, measuring orientation is not difficult since an encoder can be attached between ground and a rotating link to directly give orientation. However for any untethered system, or one that can move about freely in space, determining its orientation is not trivial. In our case, we are designing a hopping robot with a single actuator, capable of balancing despite inherent open-loop instability [6]. This robot requires accurate orientation and rate feedback at a relatively high bandwidth in order to achieve stable balance control. In this paper we develop a state-space estimation approach that meets these requirements using inexpensive components. We focus our attention on planar motions, since sensing in 3-dimensions first requires sensing in the plane [7].

One option for planar orientation measurement is the use of a tilt sensor, such as a pendulum type inclinometer, but these sensors have their own dynamics with limited bandwidth and therefore cannot provide the correct tilt information at high frequencies. Another approach is to use a gyroscope to infer the tilt angle of the robot. In theory, integrating the angular velocity output of a gyroscope (hereafter referred to as a gyro or rate gyro) should provide an accurate tilt angle, even when the system is moving or oscillating quickly. In practice, low-cost gyros have an unknown bias (offset) and/or scaling in their output, as well as signal noise. Integrating the gyro output results in a angle estimate plus a drift term. This means that it is not practical to sense inclination angle from a gyro alone.

Another approach is to use a 2-axis accelerometer to measure the direction of gravity in a rotating reference frame [8]. Because accelerometers have a relatively high bandwidth and low cost, they are often used in this manner as tilt sensors. In practice, however, we have found them to be sensitive to vibrations, and relatively difficult to use since they require a nonlinear arctangent evaluation in the control loop. Ojeda and Borenstein [5] have used accelerometers as tilt sensors to reset their gyros when their robot is not moving. They also found that vibrations during motion were problematic.

Our approach uses a state estimator which combines data from a gyro and a pendulum inclinometer to estimate the tilt angle. We used a US Digital T2-7200-T optical inclinometer (cost $\approx$ \$100) [1], along with a Murata ENC-03JA piezo gyroscope (cost $\approx$ \$50) [2], as shown in Figure 1. At first glance, our approach is similar to that used by Baerveldt and Klang [3] and by Rehbinder and Hu [4]. However, we found that none of the existing methods produced the accuracy or bandwidth that we required. Baerveldt and Klang assume the inclinometer is a first order low-pass filter, and tune the cutoff frequency by hand. This model is good for lower frequency motions (in their case 0 to 1.5 Hz), but the first order assumption is not valid at higher frequencies. Also, Rehbinder and Hu use a more sophisticated nonlinear observer to estimate attitude, but also model their inclinometer as a first order low-pass filter. Again their system operates at frequencies around 1 Hz. Because our robot systems potentially operate at frequencies approaching 5 Hz, we needed to develop a significantly improved state estimation technique.


Fig. 1. US Digital inclinometer (left), Murata gyroscope (right). For scale, note that the connection wires are 0.1 inch apart.

Our method has three main differences to previous approaches: (1) a higher fidelity model for the inclinometer was developed using both a physics-based model and a frequency domain system identification techniques and (2) an optimal state estimator (Kalman filter) is used that continuously combines the measurements to obtain more accurate angle and angular rate measurements. In addition to these state estimates, the inherent bias of the gyroscope is identified and compensated for on-line.

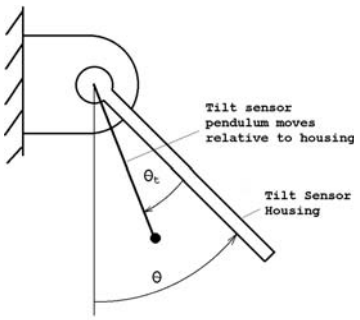


Fig. 2. A schematic for modeling the inclinometer as a simple pendulum.

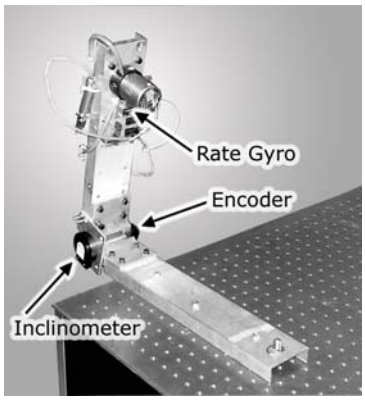


Fig. 3. Test apparatus for encoder, inclinometer, gyroscope. A chirp test signal was applied to the hardware by a pneumatically actuated controller.

## II. MODELING AND PERFORMANCE CHARACTERISTICS OF THE SENSORS

### A. Inclinometer

The US Digital optical inclinometer measures the angular position of a pendulum relative to its housing. An encoder with a resolution of 7200 counts/revolution (after quadrature) is used to track the position of the pendulum. Figure 2 shows a schematic representation of the inclinometer. Because the pendulum has its own dynamics, the desired inclination angle, $\theta_t$, output from this sensor is only accurate at low frequencies. In order to investigate the dynamics of our inclinometer, we mounted a hinge joint to a fixed table (see Figure 3) and measured the true angle of the pendulum with an optical encoder. We then oscillated the joint with an increasing frequency "chirp signal." The chirp input starts at 0.25 Hz and ends at approximately 4.6 Hz over a period of 107 seconds. Sensor outputs were sampled at 500 Hz. Figure 4 shows the output of the inclinometer as a function of time as the actual inclination angle (measured with an encoder used for comparison only) varies with the increasing frequency chirp. At high frequencies, the inclinometer exhibits distortion in both magnitude and phase.

Considering the tilt sensor to be a simple pendulum with

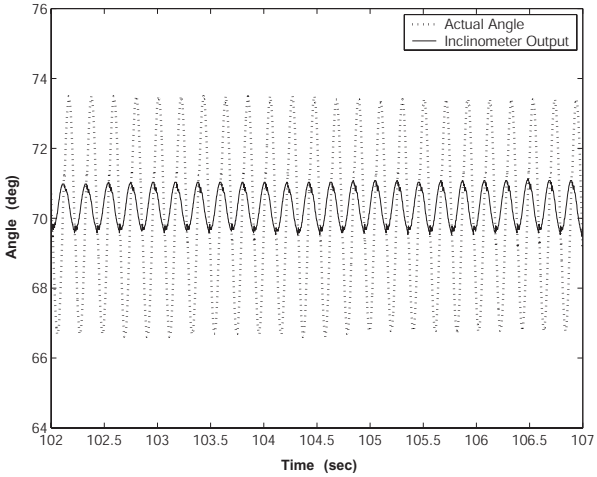


Fig. 4. Tilt angle measured with encoder and inclinometer in a chirp motion. Last 5 seconds (high frequency content) of data shown.

damping, where $\theta$ is the actual angle and $\theta_t$ is the tilt sensor output, as seen in Figure 2, the differential equation is

$$J(\ddot{\theta} - \ddot{\theta}_t) = c\dot{\theta}_t - mgl\sin(\theta - \theta_t)$$

for some damping coefficient $c$, length $l$, mass $m$, and inertia $J$. Assuming small $\theta - \theta_t$, $\sin(\theta - \theta_t) \approx \theta - \theta_t$, the transfer function for this system has the form

$$G(s) = L\left[\frac{\theta_t(t)}{\theta(t)}\right] = \frac{s^2 + mgl/J}{s^2 + c/Js + mgl/J}. \qquad (1)$$

### B. Gyroscope

In order to investigate the dynamic characteristics of the Murata gyroscope, we mounted it to the same test apparatus as used for the inclinometer experiments and applied the same chirp test signal. The raw output voltage of a Murata gyro is shown in the plots of Figure 5. This voltage has been scaled to have units comparable to rad/sec. Also shown in the figure is the signal obtained from a backward finite difference of the joint encoder signal. This signal was also passed through a first-order low-pass filter with a bandwidth of 20 Hz. From the plots, it appears that a bias of about 3 rad/sec is present in the gyro output signal. We assumed this bias was constant, subtracted it from the gyro signal, and integrated it to obtain the plots shown in Figure 6. The plots show a significant error in magnitude from the true angle (as measured by the encoder). It is clear that the gyro sensor introduces an amplification to the signal in addition to the bias drift signal.

## III. OBSERVER DESIGN FOR ACCURATE TILT MEASUREMENT

In this section, we construct an optimal observer (Kalman filter) that considerably improves tracking of the tilt angle $\theta$ by combining the inaccurate measurements of the gyro and tilt sensors. The observer reconstructs the states of the gyro/inclinometer measuring system depicted in Fig. 5. In

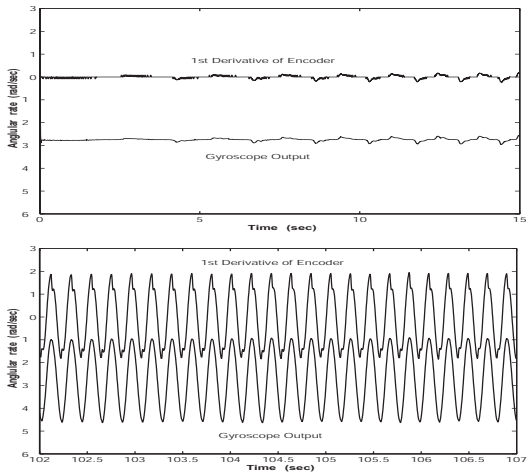


Fig. 5. The raw output from the gyroscope, and the differentiated and filtered output of the encoder at low (top) and high (bottom) frequencies.

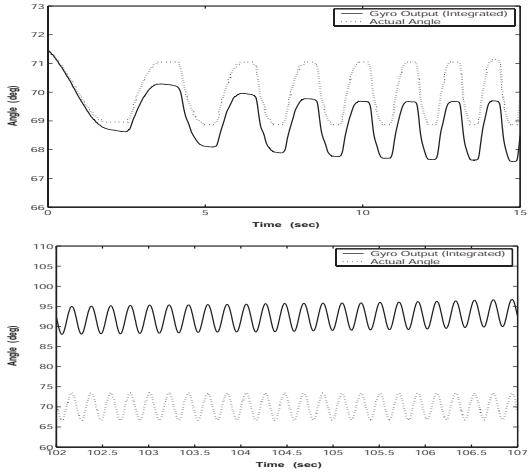


Fig. 6. The integral of the gyro signal minus a constant drift and the joint encoder signals at low (top) and high (bottom) frequencies.

this system, the tilt sensor is described by the 2nd order transfer function (1). A minimal state space realization for (1) can be assumed as follows:

$$\begin{bmatrix} \dot{x}_1 \\ \dot{x}_2 \end{bmatrix} = \begin{bmatrix} a_{11} & a_{12} \\ a_{21} & a_{22} \end{bmatrix} \begin{bmatrix} x_1 \\ x_2 \end{bmatrix} + \begin{bmatrix} b_1 \\ b_2 \end{bmatrix} \theta$$

$$\theta_t = \begin{bmatrix} c_1 & c_2 \end{bmatrix} \begin{bmatrix} x_1 \\ x_2 \end{bmatrix} + d\ \theta + v_t. \tag{2}$$

In (2), $a_{11}, a_{12},\ a_{21},\ a_{22},\ b_1,\ b_2,\ c_1,\ c_2$, and $d$ are real constants that are determined via a frequency response system identification procedure explained in Subsection III-A, and $v_t$ represents the inclinometer measurement noise. Next, the gyro sensor is described by the equation:

$$\omega_g = \frac{1}{\alpha}(\omega + \delta) + v_g \tag{3}$$

where $\omega$ and $\omega_g$ are actual and measured angular velocities and $\delta$, $\alpha$ are the bias and scaling constants in the gyro sensor respectively, and $v_g$ represents the gyro measurement noise. Finally, to model the gyro bias, we use the equation:

$$\dot{\delta} = v_b. \tag{4}$$

In (4), $v_b$ is white noise that is introduced in the model mainly for the optimal observer problem to be well-posed and solvable; however, it also allows the gyro bias to fluctuate to some extent, consistently with our experience in practice.

The above equations together with the relation

$$\dot{\theta} = \omega,$$

give the following state-space equations for the gyro/inclinometer measuring system.

$$\begin{bmatrix} \dot{\delta} \\ \dot{\theta} \\ \dot{x}_1 \\ \dot{x}_2 \end{bmatrix} = \begin{bmatrix} 0 & 0 & 0 & 0 \\ -1 & 0 & 0 & 0 \\ 0 & b_1 & a_{11} & a_{12} \\ 0 & b_2 & a_{21} & a_{22} \end{bmatrix} \begin{bmatrix} \delta \\ \theta \\ x_1 \\ x_2 \end{bmatrix} + \begin{bmatrix} 0 \\ \alpha \\ 0 \\ 0 \end{bmatrix} \omega_g + \begin{bmatrix} 1 & 0 \\ 0 & -\alpha \\ 0 & 0 \\ 0 & 0 \end{bmatrix} \begin{bmatrix} v_b \\ v_g \end{bmatrix}$$

$$\theta_t = \begin{bmatrix} 0 & d & c_1 & c_2 \end{bmatrix} \begin{bmatrix} \delta \\ \theta \\ x_1 \\ x_2 \end{bmatrix} + v_t.$$

This system is of the standard form:

$$\begin{aligned} \dot{z} &= A\ z + B\ \omega_g + B_v\ v \\ \theta_t &= C\ z + v_t \end{aligned}$$

with $z \equiv [\delta\ \theta\ x_1\ x_2]^T$, $v \equiv [v_b\ v_g]$, and $A$, $B$, $B_v$, and $C$ defined in an obvious way. Note that in this formulation, the unknown bias $\delta$ and the tilt angle $\theta$ are states of the system. The inputs are the measured gyro signal $\omega_g$ and the measurement noises $v_b$, $v_g$, and $v_t$. Finally, the output of the system is the measured inclinometer signal $\theta_t$. Next, we consider a standard state estimator (observer) of the form:

$$\dot{\hat{z}} = A\ \hat{z} + K\ (\theta_t - C\ \hat{z}) + B\ \omega_g \tag{5}$$

Selecting the gain vector $K$ such that $A - KC$ is an asymptotically stable matrix guarantees that the state reconstruction error $z - \hat{z}$ remains bounded, and in the absence of the noise signals, that $z - \hat{z}$ converges asymptotically to 0. We actually considered an optimal observer (Kalman filter) that minimizes the mean square tracking error $E[(z - \hat{z})^T(z - \hat{z})]$ and can be readily designed by considering the dual state regulator problem (for example, see [9]) and using MATLAB's *lqr* command. In the cost function of the latter problem, the state weighting matrix $Q = \mathrm{diag}\left\{W_b^2,\ \alpha^2\ W_g^2,\ 0,\ 0\right\}$ and the control weighting matrix $R = W_t^2$, where $W_b$, $W_g$, and $W_t$ are the RMS (root mean square) values of the bias $v_b$, gyro $v_g$, and tilt sensor $v_t$ noises respectively, all assumed to be modelled as white noise. The values of $W_b^2$, $W_g^2$, and $W_t^2$ are actually used to tune the performance of the observer,

namely, to trade-off the speed of state reconstruction with the extent of observer bandwidth and its susceptibility to measurement noise. We found that the values $W_b = 1$, $W_g = 0.001$, and $W_t = 0.001$ provide a reasonable such trade-off, and resulted in the observer gains $K = [-31.6228\ 11.0784\ 0.4324\ 3.6152]^T$.

### A. System Identification of Inclinometer Dynamics

From (5), it is clear that the observer acts as a filter that combines the imperfect gyro $\omega_g$ and inclinometer $\theta_t$ signals to produce an improved estimate of the tilt angle $\theta$ in terms of the estimated state $\hat{z}(2)$. Note that the observer, automatically estimates the gyro bias $\delta$ in terms of $\hat{z}(1)$ and compensates for it. However, in order to use this scheme, we need to have the observer parameters $a_{ij}$, $b_i$, $c_i$, and $d$, or equivalently to identify the inclinometer transfer function in (1). We employ a frequency domain identification technique to do this. More specifically, the output of the integrator/inclinometer system in Fig. 5 is the inclinometer measurement $\theta_t$, while the input to this system (neglecting measurement noise) is $\omega$, that from (3) is related to the gyro measurement $\omega_t$ by:

$$\omega = \alpha\ \omega_g - \delta.$$

For the moment, we assume that $\delta = 0$ and $\alpha = 1$, i.e. that $\omega = \omega_g$ and we will shortly see that the value of the bias $\delta$ does not affect the identification process, while the actual scaling $\alpha$ can be easily determined through this process. The measured signals $\omega_g$ and $\theta_t$ are produced by applying a chirp input as discussed in Section II-A. Over the time horizon $T = 107$ sec with a sampling frequency $f = 500Hz$, we collected $N = 53501$ samples. We then computed the Discrete Fourier Transforms (DFT) of $\omega_g(k\ T_p)$ and $\theta_t(k\ T_p)$, $k = 0, \ldots, 53500$, where $T_p = 1/f = 0.002$ sec using MATLAB's *fft* command. Finally, we obtained samples of the integrator/inclinometer frequency response $G(jk\Omega_p)$, $k = 0, \ldots, 53500$, where $\Omega_p = \frac{2\pi}{T} = 0.0093$ rad/sec, as the ratio of the DFT of $\theta_t$ to the DFT of $\omega_g$. We should remark that a number of factors contribute to errors in the estimation of the samples $G(jk\Omega)$. First, since the chirp input has its power over frequencies from $0.25Hz$ to $4.6Hz$, we can expect to be able to reliably identify the frequency range from about $0.2Hz$ to $5Hz$. Then, errors may be introduced because of aliasing and leakage [10]. However, we do not expect aliasing to be a factor since we used an anti-aliasing filter with a cutoff frequency of 50 Hz. This means that our sampling rate of $500Hz$ is 10 times higher than the expected bandwidth of the signals being sampled. Leakage is the ripple effect on the frequency response created by using a finite horizon time sequence instead of an infinite one. It can be reduced by increasing $N$, or by using windowing filters at the expense of smearing the frequency response. Indeed, since we did not employ any data windowing, some rippling in the frequency samples can be observed but the curve fitting approach we use tends to smooth out this effect. Next, the experimental frequency response curve (samples $G(jk\Omega)$) is fitted with a rational transfer function by minimizing a least squares criterion:

$$\min_{a_k,\ b_l} \sum_{i=N_1}^{N_2} w_i \left| G(j\Omega_i) - \frac{b_m(j\Omega_i)^k + \ldots + b_0}{a_n(j\Omega_i)^k + \ldots + a_0} \right|^2 \qquad (6)$$

with $k = 0, \ldots, n$ and $l = 0, \ldots, m$. In (6), the $w_i$s are weights that are selected to tune the approach. We employed a recursive algorithm reported in [11], with the additional parametrization of the numerator and denominator polynomials of the fit in terms of Chebychev polynomials to alleviate numerical difficulties as reported in [12] and [13]. As discussed above, we took $N_1$ and $N_2$ in (6), to fit the available data from $0.2Hz$ to $5Hz$. Furthermore, to obtain an exact integrator $(1/s)$ behavior at low frequencies, we first scaled the experimental frequency response samples by $s$; then the resulting transfer function describes exactly the inclinometer dynamics.

We now remark on why the gyro bias $\delta$ does not affect this procedure and how the scaling $\alpha$ can be accurately determined. First note that the bias introduces a delta function at $s = 0$ in the frequency response and that curve-fitting is attempted from $0.2Hz$ to $5Hz$ so that the bias has no effect on the identification. Then, note that $\alpha$ has the effect of scaling the experimental frequency response and the curve-fit. Since it is known that the dc-gain of the inclinometer is 1, we simply identify $\alpha$ as the scaling required to make the resulting curve-fit have a dc-gain of 1.

Figure 7 shows the best-fit transfer functions of varying degrees, starting with 1 pole and no zeros (top left), 2 pole and no zeros (top right), and 2 poles and 2 zeros (bottom). Note that the first order model, seen in Figure 7, can stay in phase with the data fairly well, but suffers from magnitude roll-off at frequencies exceeding 1 Hz. The bottom plot in the figure shows an excellent fit within the 0.2 to 5Hz range, The identified the transfer function for the inclinometer is:

$$G(s) = \frac{1.024s^2 - 0.1791s + 528.4}{s^2 + 65.86s + 528.4}.$$

We observe, that $G_p(s)$ is consistent with our theoretical analysis, less the small damping in the numerator that can be attributed mainly to the finite resolution in our samples. We also remark that the natural frequency of the zeros of the model is $\frac{\sqrt{528.4}}{2\pi} = 3.66Hz$, well within the range of device, which shows the importance of using the more accurate model. Finally, the gyro scaling is identified to have a value of $\alpha = 0.76$ based on the approach discussed above.

### B. Experimental Results

Figure 8 shows the estimated tilt angle by the observer designed as explained in Subsection III and based on the inclinometer parameters identified as discussed in Subsection III-A. The observer output is compared to the actual angle (measured separately by an encoder for the purpose of comparison) at low and high frequencies. Note that the observer, given arbitrary initial conditions, converges to the

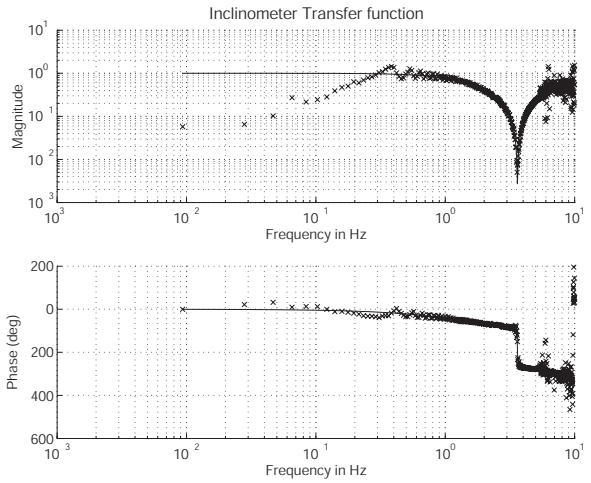


Fig. 7. Best-fit transfer function with 2 poles and 2 zeros.

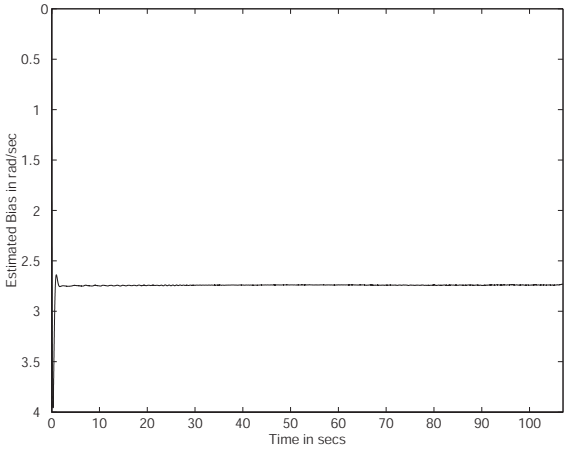


Fig. 9. The observer's estimate of the gyro bias during the chirp motion.

encoder signal in about 2 seconds. The last 5 seconds of the chirp motion show our observer tracking a signal of frequencies exceeding 4 Hz. Figure 9 shows the estimate of the gyro bias signal to quickly converge to a value of $\delta = -2.74$ deg/sec.

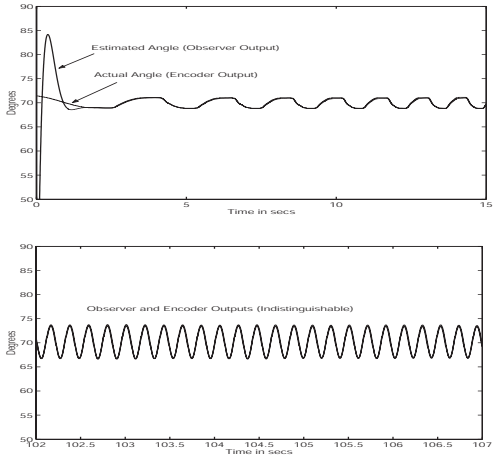


Fig. 8. Observer designed from tilt sensor transfer function, 2 poles and 2 zeros (top–first 15 sec, bottom–last 5 sec).

## IV. Effect of moving tilt sensor away from rotation center

The model seen in (1) is only good for the case when the inclinometer rotates without translating. If the inclinometer is placed away from the axis of rotation, the sensor will translate as well as rotate, and a new model is required. In this case, one might develop a non-linear physical model and linearize it around a typical operating point. However, the linearized model can be found experimentally by finding a transfer function that fits the frequency response of the system. In other words, one can identify the linearized model using the same methods as Section III-A, without taking the physical model into account. Figure 10 compares the frequency response of our best-fit model (a 2 pole, 1 zero transfer function) to the experimental response. Notice that a first order model would be incapable of fitting this high-pass type frequency response.

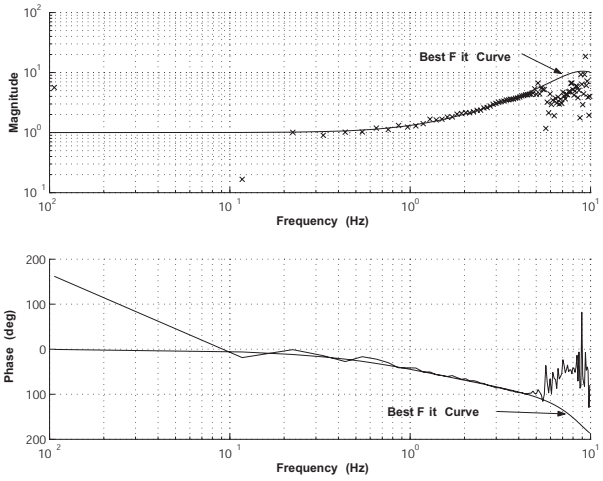


Fig. 10. Best-fit transfer function with 2 poles and 1 zero, using data from an inclinometer that has been displaced from the axis of rotation

Figure 11 shows the results of the observer we designed with our identified second order model. The observer tracks the actual angle well at low and high frequencies, although not as closely as before. This is because the nonlinear acceleration of the inclinometer has more of an effect on the errors in our linear observer. An important feature of our system identification technique used in this section and in Section III-A is that it can be applied to untethered systems, since no encoder is needed for the system identification. It can also potentially be done on-line.

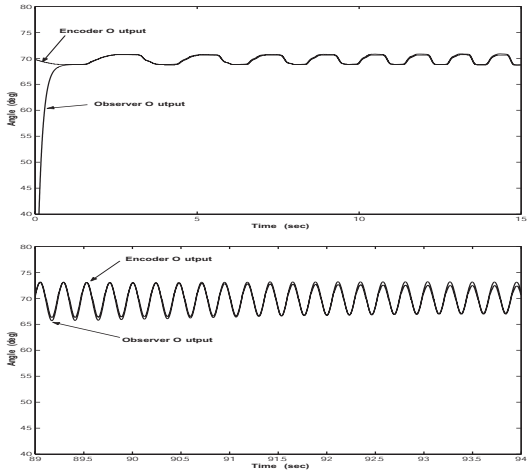


Fig. 11. Observer designed from tilt sensor transfer function (sensor away from center of rotation), 2 poles and 1 zero (top–first 15 sec, bottom–last 5 sec).

## V. CONCLUSION

We have outlined a method for combining data from 2 inexpensive sensors, an inclinometer and a rate gyro, to produce an accurate angle measurement for high bandwidth signals. The rate gyro is modeled as the derivative of the angle to be estimated, plus an unknown constant bias. The tilt sensor is modeled as a second-order proper transfer function from the actual angle to the tilt sensor output. The parameters of this transfer function are obtained by fitting its frequency response to the experimental frequency response of the tilt sensor to a chirp motion. Then, an optimal linear state estimator is constructed that estimates the gyro bias, and infers the correct angle from the output of both sensors. Although not shown in this paper, our method removes the gyro bias more effectively than the analog high-pass filter suggested by the manufacturer. Furthermore, our more realistic model of the inclinometer allows for state observation at higher frequencies than has been reported in previous research.

## REFERENCES

[1] US Digital Corporation. Part Number: T2-7200-T
[2] Murata Manufacturing Co., Ltd. Part #: ENC-03JA.
[3] A.J. Baerveldt and R. Klang, "A Low-cost and Low-weight Attitude Estimation System for an Autonomous Helicopter," *IEEE Conference on Intelligent Engineering Systems, Proceedings*, 1996 pp. 391-395
[4] H. Rehbinder and X. Hu, "A nonlocal nonlinear observer for rigid body motion with low-pass sensors," *Mathematical Theory of Networks and Systems*, Perpignan, 2000.
[5] L. Ojeda and J. Borenstein, "FLEXnav: Fuzzy Logic Expert Rule-based Position Estimation for Mobile Robots on Rugged Terrain," *Proceedings of the 2002 IEEE International Conference on Robotics and Automation, Washington DC, USA*, 11 - 15 May 2002, pp. 317-322.
[6] J.Leavitt, "Robust Balance Control of an Under-Actuated, One-Legged Hopping Robot", Master of Science Project Report, University of California, Irvine, 2003.
[7] H.J. Luinge et al, "Estimation of orientation with gyroscopes and accelerometers," *Engineering in Medicine and Biology, 1999. 21st Annual Conf. and the 1999 Annual Fall Meeting of the Biomedical Engineering Soc. BMES/EMBS Conference, 1999. Proceedings of the First Joint* , vol 2 , 13-16 Oct. 1999 p. 844.
[8] J. Vaganay et al, "Mobile robot attitude estimation by fusion of inertial data," *IEEE International Conference on Robotics and Automation, Proceedings* , 2-6 May 1993, vol. 1, pp 277 -282.
[9] H. Kwakernaak and R. Sivan, *Linear Optimal Control Systems*, Wiley-Interscience, New York, NY; 1972.
[10] E. Brigham, *The Fast Fourier Transform and its Applications*, Prentice Hall, Englewood Cliffs, NJ, 1988.
[11] C.K. Sanathanan and J. Koerner, *IEEE Transactions on Automatic Control*, vol. 8 issue 1 , Jan 1963, pp 56-58.
[12] J.L. Adcock, "Analyzer Synthesizes Frequency Response of Linear Systems," *Hewlett-Packard Journal*, Jan 1987, pp 25-32.
[13] J.L. Adcock, "Curve Fitter for Pole-Zero Analysis," *Hewlett-Packard Journal*, January 1987, pp 33-36.